Supporting Information

Shen et al. 10.1073/pnas.1712555114

SI Materials and Methods

Fatty Acid Solution. Palmitic acid (16:0), stearic acid (18:0), oleic acid (18:1), palmitic acid-d_{31} (98% D), stearic acid-d_{35} (98%D), and oleic acid-d_{34} (98% D) were from Sigma. Lauric acid-d_{23} (98% D) (12:0) and myristic acid-d_{27} (98% D) (14:0) were from Cambridge Isotope Laboratory. Fatty acids were reacted with sodium hydroxide (Sigma) above melting point to form 20 mM solution, and then coupled to fatty-acid–free BSA (Sigma A7030) in about 2:1 molar ratio to make 2 mM stock solution in culture medium. They were then added to cell culture to achieve the designated concentration. Four hundred micromolar fatty acid was used in this study, if not specified. For extremely low concentration (10 and 20 μM), serum was reduced from 10 to 1% to minimize interference from serum fatty acid. Control cells were treated with only BSA of the same concentration.

Cell Culture. HeLa (ATCC) and COS-7 (ATCC) were maintained in DMEM (Invitrogen; 11965-092), supplemented with 10% FBS (16000-044; Invitrogen) and 100 U/mL penicillin-streptomycin (15140-122; Invitrogen). Triacsin C (Sigma), as an inhibitor of acyl-CoA synthetase, was made into 25 mM stock solution in DMSO. Cells that reached 80% confluence were dissociated and plated onto coverslips (No. 1; Fisher Brand) for most experiments and glass-bottom Petri dish (P35G-1.5-14-C; MatTek) for experiments with single-cell tracking. The coverslip was stuck to a microscope slide (1 mm thick; VWR) using 0.1-mm imaging spacer (SecureSeal) to make an imaging chamber filled with PBS.

Transfection. Scrambled siRNA (4390843; Thermo Fisher) or GPAT4 siRNA (s44067; Thermo Fisher) was transfected by Lipofectamine RNAiMax (Thermo Fisher) according to the manufacturer's procedure. The ER is visualized in live cells using CellLight ER-GFP (Thermo Fisher Scientific) according to the manufacturer's manual. mCherry-Sec61β was a gift from Gia Voeltz, University of Colorado Boulder, Boulder, CO (Addgene; plasmid # 49155). Cherry-LiveDrop, as described earlier (1), was a gift from Tobias C. Walther and Robert V. Farese, Jr., Harvard Medical School, Boston. Transient transfection was done in near-confluent HeLa cells with Lipofectamine 3000 Reagent (Thermo Fisher Scientific) at 200 ng of DNA per well in a 24-well plate. Five to 10 h after transfection, cells were split and replated to adjust cell density. Images were taken 24–48 h after transfection.

SRS Microscopy. The setup for SRS microscopy was similar to what was described earlier (2). Briefly, two spatially and temporally overlapped picosecond pulsed laser beams (Pump and Stokes) were produced by picoEmerald laser system (Applied Physics and Electronics) and directed into a laser-scanning microscope (FV1200MPE; Olympus) through a 60× objective (water immersion, N.A. 1.2, UPlanAPO/IR; Olympus). The Stokes beam was modulated by electro-optic modulator at 8 MHz to enable detection of stimulated Raman loss in pump photon after light interaction with chemical bond vibration. Transmitted Pump and Stokes beams were collected by a high N.A. condenser (oil immersion, 1.4 N.A.; Olympus), filtered by a bandpass filter (890/220 CARS; Chroma Technology) and projected onto a 10 × 10-mm^2 Si photodiode (FDS1010; Thorlabs) biased at 64 V to measure only the Pump beam intensity. The output current is terminated by a 50-Ω terminator, prefiltered at 8 MHz (±1 MHz, KR 2724; KR Electronics), and then demodulated by a lock-in amplifier (SR844; Stanford Research Systems). The in-phase X output was used to generate SRS image at the speed of 100 μs/pixel. Laser powers on sample were measured to be up to 120 mW (Stokes) and 100 mW (Pump). The wavelength of Stokes laser was 1,064 nm and wavelengths for Pump laser used in this study were as follows: 810.5 nm (2,940 cm^{-1}, mainly protein CH_3), 816.7 nm (2,845 cm^{-1}, mainly lipid CH_2), 869.0 nm (2,101 cm^{-1}, C–D on resonance), and 885.0 nm (off-resonance background). Images were acquired by Fluoview software and were later assigned pseudocolors in ImageJ.

Fluorescence Imaging. BODIPY 500/510 C_1, C_{12} (BODIPY-C_{12}) (Molecular Probes) (diluted from 10 mM stock solution in DMSO) was used as a fluorescent fatty acid tracer at 2 μM in the culture medium. Neutral lipid was stained with 1 μM Nile Red solution (diluted from 1 mM stock in DMSO) (Molecular Probes) before cells were fixed by 4% paraformaldehyde (PFA). For SERCA2a immunofluorescence, cells were fixed in 4% PFA at room temperature for 10 min, permeabilized for 30 min in PBS containing 0.1% Tween 20, 0.3 M glycine (Sigma), 10% goat serum (Invitrogen), and 1% BSA, and then incubated with mouse monoclonal antibody to SERCA2a (2A7-A1; Abcam; ab2861) at 1:1,000 dilution in 2% BSA overnight at 4 °C. They were then blocked in 10% goat serum, washed three times with PBS, then incubated with Alexa 647–goat anti-mouse IgG at 1:1,000 dilution in 10% goat serum overnight at 4 °C, and finally blocked by 10% goat serum.

Confocal fluorescence imaging was performed on the same microscope used for SRS imaging (FV1200; Olympus) and the same objective (60×, water immersion, N.A. 1.2, UPlanAPO/IR; Olympus). For BODIPY-C_{12}, Nile Red, and ER-GFP, the excitation wavelength and filter selection were 488 and 505–605 nm. For mCherry, the excitation wavelength and filter selection were 543 and 560–660 nm. For SERCA2 immunofluorescence, the excitation wavelength and filter selection were 635 and 655–755 nm. As SRS and fluorescence measurements used different lasers and dichroic mirrors, image was slightly shifted from one to the other channel. To perform multichannel colocalization, we used a standard grid to determine the offset between the field of views of SRS and fluorescence and corrected it in all of the multichannel images later. Images were acquired by Fluoview software and pseudocolored by ImageJ.

Spontaneous Raman Spectroscopy. Spontaneous Raman spectra were acquired using an upright confocal Raman spectrometer (Xplora; HORIBA Jobin Yvon), with temperature controlled by water bath (±1 °C). Samples were illuminated by 532-nm (25-mW) laser through a 100× objective (air, N.A. 0.9, MPlan N; Olympus). Reference lipids including DPPC-d_{62} and POPC-d_{31} (deuteration on palmitoyl chain; Avanti Polar Lipids) were first dissolved in 1:2 chloroform:methanol to make 50 mM solution. The solvent was then evaporated in argon gas flow, and lipids were reconstituted in PBS to 50 mM after repeated sonication until a dispersion of multilamellar vesicles was formed. Cell spectra were obtained from cells fixed with 4% PFA; lipid droplets were avoided judging by bright-field view. Glass and solution background was subtracted by measuring noncell signal near the targeted cell. For each condition, three different regions on the sample were randomly selected, and their spectra were averaged. The acquisition time was 20 s for reference lipids and 400 s for cells.

CH_2 CH_3 Unmixing Algorithm. To separate total lipid and protein signal from their overlapping spectrum, we adapted a previously reported spectral unmixing algorithm (3). Briefly, we acquired the

SRS signals from two wavelengths bearing features of lipid and protein, respectively, and the amount of the two species can be determined by a linear combination of the signal at those two wavelengths (see below), with coefficients R_1 and R_2 predetermined by pure substances. Here, signals at 2,845 and 2,940 cm^{-1} were measured to perform the spectral unmixing:

$$\text{lipid}[CH_2] = R_1 \cdot [2845] - R_2 \cdot [2940],$$

$$\text{protein}[CH_3] = [2940] - [2845],$$

$$\text{where } R_1 = 5; \quad R_2 = 0.4.$$

Note that this spectral unmixing is rather an estimation of total lipid content than a precise separation of chemical species. The unmixed lipid signal is used for C–H SRS channel in Figs. 2*D* and 5*F* and Figs. S3 and S7.

Image Segmentation for LD and Membrane Signal. Image segmentation in correlative Nile Red fluorescence and C–D SRS image sets (Fig. S4 *B* and *C*) was performed in ImageJ. Cells with isolated C–D SRS domains were selected. LDs were first segmented using an intensity threshold in Nile Red fluorescence image. The LD pixels were then left out in C–D SRS image. Resulting C–D SRS image was segmented using intensity threshold and reasonable circularity range.

Cell Viability Assay. Cells were plated in 96-well plate; after designated treatment concentration and time, cell number was quantified using CellTiter-Glo Luminescent Cell Viability Assay (Promega) following the manufacturer's instruction.

Free Fatty Acid Quantification. Cells were plated in six-well plate; after treatment with palmitate, intracellular free fatty acid was quantified by fluorometry using Free Fatty Acid Quantification Kit (Sigma) following the manufacturer's instruction. Protein concentrations were also quantified from each sample as normalization (see below).

Determination of Protein Concentration Using BCA Assay. Protein concentration was determined to quantify lipid composition in cell. Cells cultured in six-well plate were washed with ice-cold PBS for three times. They were then lysed in 100 μL of RIPA buffer on ice for 2 min before being scraped to collection tube. Cell lysates were centrifuged at 1,000 × *g* for 5 min to remove cell debris. Protein concentration in the obtained supernatant was measured using Pierce protein BCA assay kit (Thermo Fisher) following the manufacturer's instruction.

Analysis of Lipids Using HPLC-MS. Lipid extracts were prepared using a modified Bligh and Dyer procedure as described previously (4, 5), spiked with appropriate internal standards, and analyzed using a 6490 Triple Quadrupole LC/MS system (Agilent Technologies). Glycerophospholipids and sphingolipids were separated with normal-phase HPLC as described before (5), with a few modifications. An Agilent Zorbax Rx-Sil column (inner diameter, 2.1 × 100 mm) was used under the following conditions: mobile phase A (chloroform:methanol:1 M ammonium hydroxide, 89.9:10:0.1, vol/vol) and mobile phase B (chloroform:methanol:water:ammonium hydroxide, 55:39.9:5:0.1, vol/vol); 95% A for 2 min, linear gradient to 30% A over 18 min and held for 3 min, and linear gradient to 95% A over 2 min and held for 6 min. Sterols and glycerolipids were separated with reverse-phase HPLC using an isocratic mobile phase as before (5) except with an Agilent Zorbax Eclipse XDB-C18 column (4.6 × 100 mm). Quantification of lipid species was accomplished using multiple-reaction monitoring transitions that were developed in earlier studies (5) in conjunction with referencing of appropriate internal standards: PA 14:0/14:0, PC 14:0/14:0, PE 14:0/14:0, PI 12:0/13:0, PS 14:0/14:0, SM d18:1/12:0, D_7-cholesterol, CE 17:0, MG 17:0, 4ME 16:0 diether DG, D_5-TG 16:0/18:0/16:0 (Avanti Polar Lipids).

Estimation of d-Palmitoyl (d_{31}-Labeled) Number from C–D SRS Intensity. To estimate number of d_{31}-palmitoyl group, we first obtained a concentration curve (Fig. S9) by measuring C–D SRS intensity of d_{31}-palmitic acid solution in DMSO with varying concentration. Linear fitting of the concentration curve yielded a slope of 1.64 μV/mM.

The average intensity spacing calculated for HeLa cell is 15 μV. This corresponds to number of d_{31}-palmitoyl groups ($N_{\text{d-palmitoyl}}$) as calculated below:

$$N_{\text{d-palmitoyl}} = \frac{\text{step size}}{\text{slope}} \cdot \text{focal volume} \cdot N_A,$$

$$= \frac{15\ \mu V}{1.64\ \mu V/mM} \cdot \pi \cdot (300\ nm)^2 \cdot 2\ \mu m \cdot 6.02 \times 10^{23} = 3.1 \times 10^6,$$

where N_A is the Avogadro constant, and focal volume is approximated by a cylinder whose radius and height are 300 nm and 2 μm, respectively.

The number of palmitoyl groups in a DPPC bilayer within focal area ($N_{\text{palmitoyl, DPPC}}$) can also be estimated. The area per DPPC molecule occupies is estimated to be 50 $Å^2$ (6). Thus,

$$N_{\text{palmitoyl,DPPC}} = \frac{\text{focal area}}{\text{area per molecule}} \cdot 2\ \text{layers} \cdot 2\ \text{palmitoyl per molecule},$$

$$= \frac{\pi \cdot (300\ nm)^2}{50\ Å^2} \cdot 2 \cdot 2 = 2.3 \times 10^6.$$

Thus, $N_{\text{d-palmitoyl}}$ calculated from image intensity is very close to $N_{\text{palmitoyl, DPPC}}$, which suggests that the structures in SRS C–D channel are composed of layered membrane.

Estimation of Diffusion Coefficient (*D*) in Individual Membrane Domain. We carried out estimation by assuming diffusion pattern was established after initiation in the center point. In reality, after the first period of d-palmitate or d-stearate labeling in sequential pulse-chase experiment, the C–D species formed a disk in the center, and point spread function also contributes to the widening of the intensity distribution. Therefore, our calculation results would be an overestimation.

For two-dimensional diffusion, the intensity (I) distribution along radius after diffusion time t can be fitted into a Gaussian curve:

$$I(r,t) \propto e^{-\frac{r^2}{4Dt}}.$$

For example, in this study, t = 3,600 s, Gaussian fitting of the central peak in the line profiles (Fig. 5 *C* and *D*) yielded $4Dt \sim 2\ \mu m^2$, so $D \sim 10^{-4}\ \mu m^2/s$.

1. Wang H, et al. (2016) Seipin is required for converting nascent to mature lipid droplets. *eLife* 5:1–28.
2. Wei L, et al. (2014) Live-cell imaging of alkyne-tagged small biomolecules by stimulated Raman scattering. *Nat Methods* 11:410–412.
3. Yu Z, et al. (2012) Label-free chemical imaging in vivo: Three-dimensional non-invasive microscopic observation of amphioxus notochord through stimulated Raman scattering (SRS). *Chem Sci* 3:2646–2654.
4. Bligh EG, Dyer WJ (1959) A rapid method of total lipid extraction and purification. *Can J Biochem Physiol* 37:911–917.
5. Chan RB, et al. (2012) Comparative lipidomic analysis of mouse and human brain with Alzheimer disease. *J Biol Chem* 287:2678–2688.
6. Kučerka N, Nieh M-P, Katsaras J (2011) Fluid phase lipid areas and bilayer thicknesses of commonly used phosphatidylcholines as a function of temperature. *Biochim Biophys Acta* 1808:2761–2771.
7. de Almeida RFM, Fedorov A, Prieto M (2003) Sphingomyelin/phosphatidylcholine/cholesterol phase diagram: Boundaries and composition of lipid rafts. *Biophys J* 85:2406–2416.
8. Cullis PR, Fenske DB, Hope MJ (2008) *Biochemistry of Lipids, Lipoproteins and Membranes* (Elsevier, Amsterdam), 5th Ed, pp 1–37.

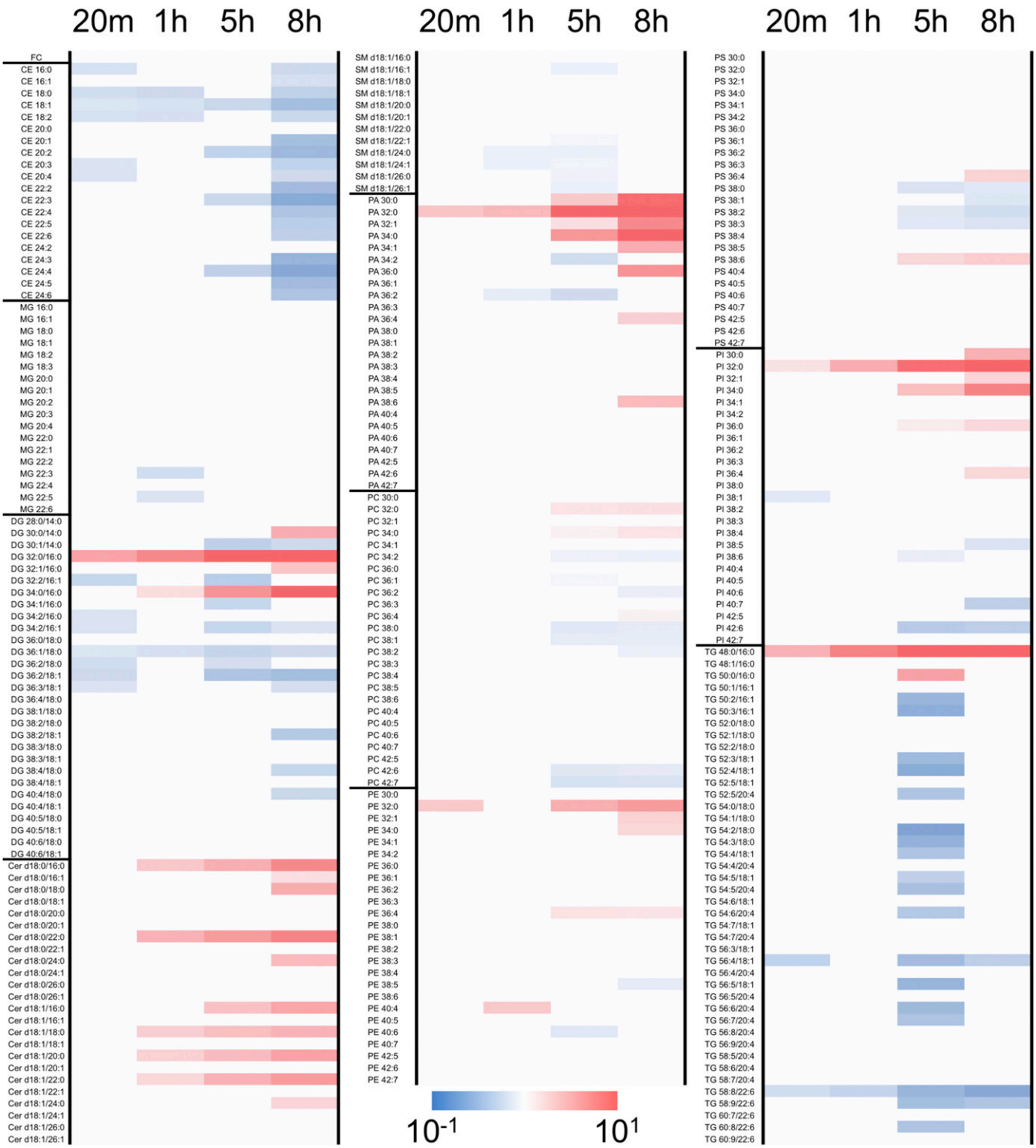

Fig. S1. Alterations in major lipids after treatment by palmitate for 20 min, 1 h, 5 h, and 8 h. Fold change ($P < 0.05$, Student's *t* test) was calculated and shown in the heat map. CE, Cholesterol ester; Cer, ceramide; DG, diacylglyceride; MG, monoacylglyceride; PA, phosphatidic acid; PC, phosphatidylcholine; PE, phosphatidylethanolamine; PI, phosphatidylinositol; PS, phosphatidylserine; SM, sphingomyeline; TG, triacylglyceride.

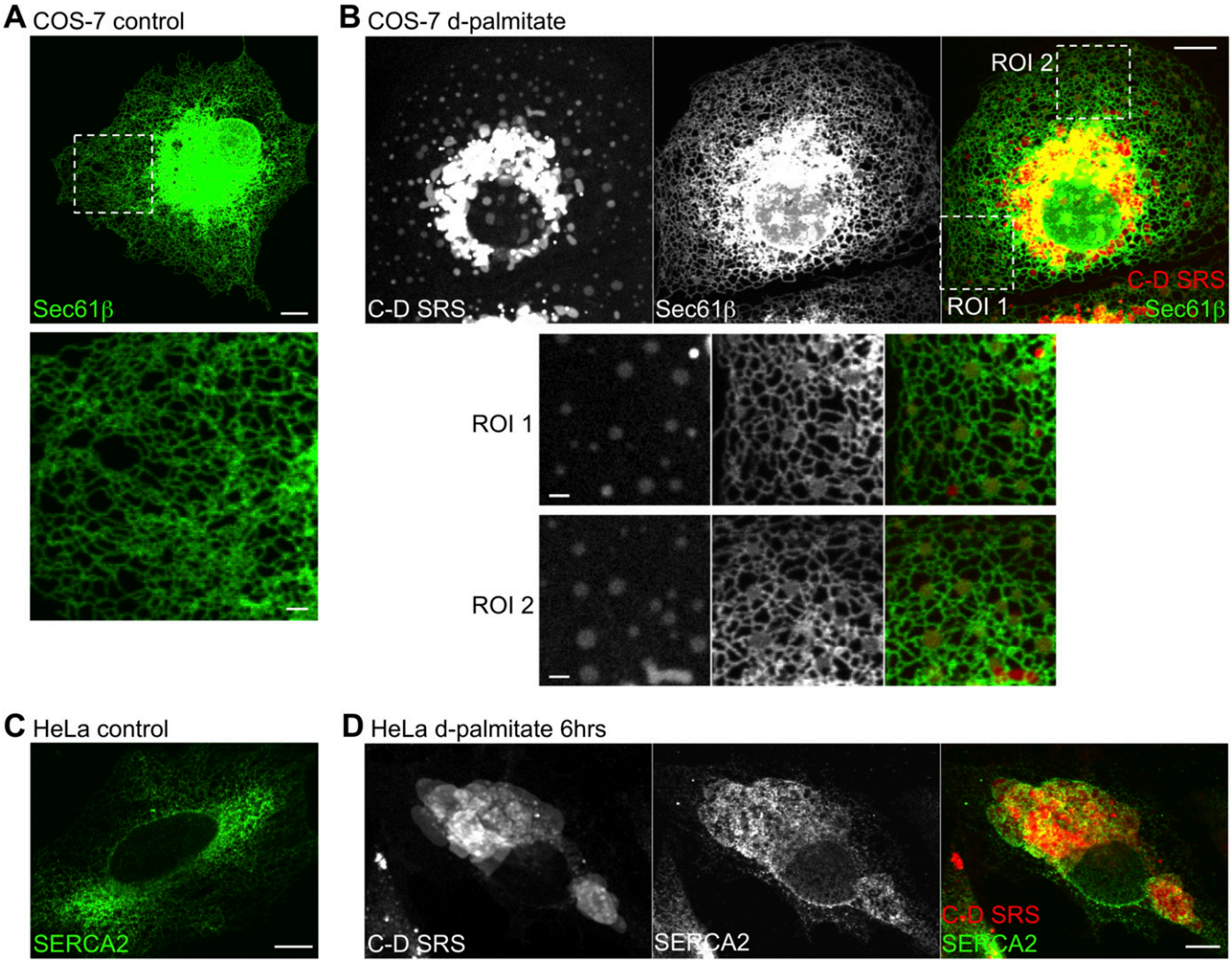

Fig. S2. Palmitate-derived structures colocalize with ER markers. mCherry-Sec61β–expressing COS-7 cell, control (*A*) and treated with d-palmitate for 4 h (*B*). Magnified views are shown for boxed areas. SERCA2 immunofluorescence in HeLa cell, control (*C*) and treated with d-palmitate for 6 h (*D*). (Scale bars: major, 10 μm; *Inset*, 2 μm.)

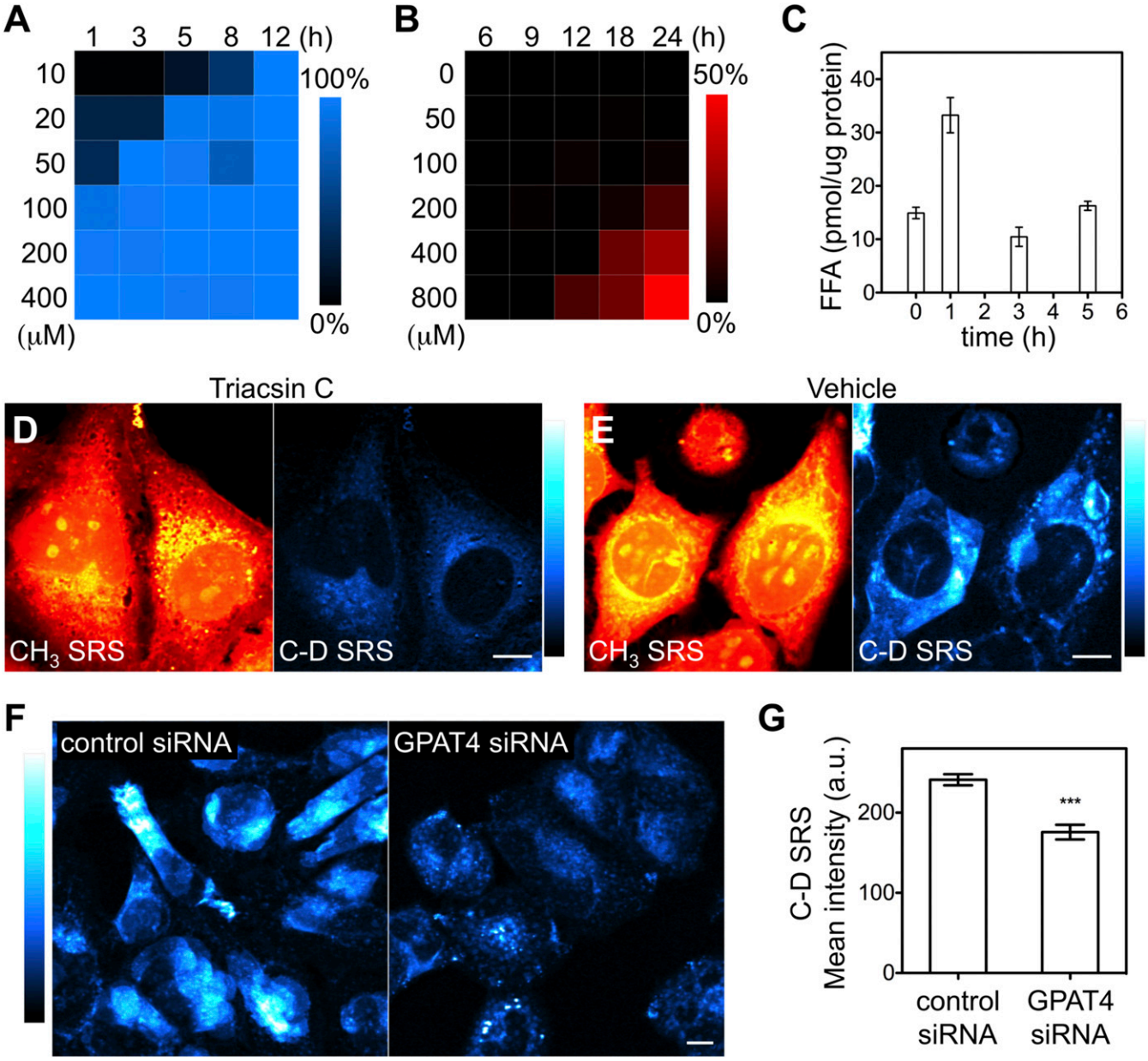

Fig. S3. Palmitate-derived structure is a result of lipid synthesis. (*A*) Percentage of cells with observable palmitate-derived non-LD structure. (*B*) Time- and dose-dependent decrease in cell number after treatment with palmitate. (*C*) FFA concentration measured in HeLa cells after treatment by palmitate for 0, 1, 3, and 5 h. Data are presented as mean ± SEM; $n = 4$. (*D* and *E*) HeLa cells were treated with d-palmitate for 5 h in the presence of 5 μM Triacsin C (*D*) or vehicle (DMSO) (*E*). CH_3 SRS shows total protein distribution as morphology of the cell. (*F*) HeLa cells transfected with control siRNA or GPAT4 siRNA for 48 h, and treated with d-palmitate for 6 h. Representative C–D SRS images are shown. (*G*) Mean C–D SRS intensity is quantified for each condition. $P < 0.001$; $n = 4$; total cell number >100. (Scale bars: 10 μm.)

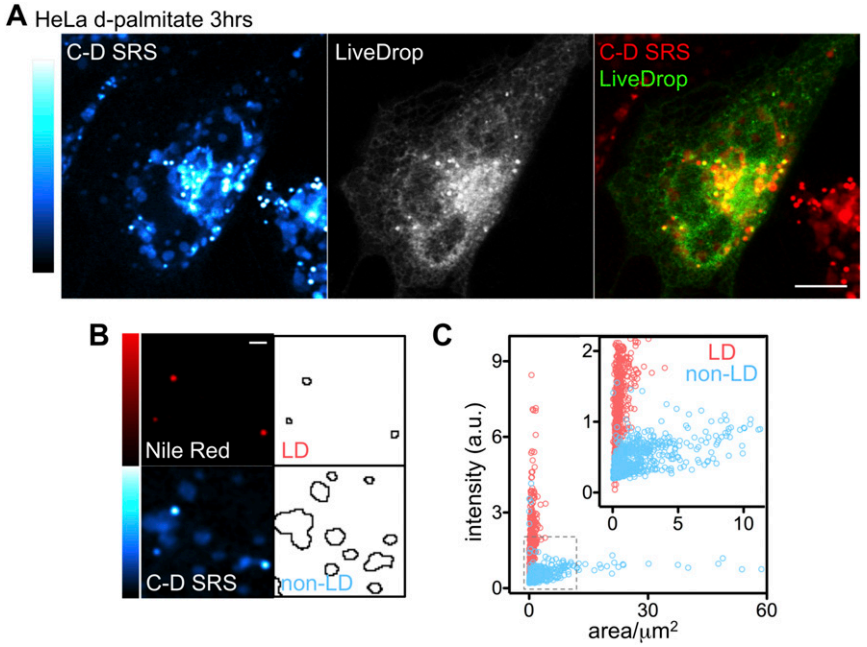

Fig. S4. Image quantification and analysis reveals membrane features of palmitate-derived structure. (*A*) HeLa cell expressing cherry-LiveDrop (nascent lipid droplet) treated with d-palmitate for 3 h. (*B*) Representative images showing image segmentation based on Nile Red positive (LD) or Nile Red negative (non-LD). (*C*) C–D SRS intensity quantification and area measurement from LD and non-LD signal based on segmentation in *B*. (Scale bars: major, 10 μm; *Inset*, 2 μm.)

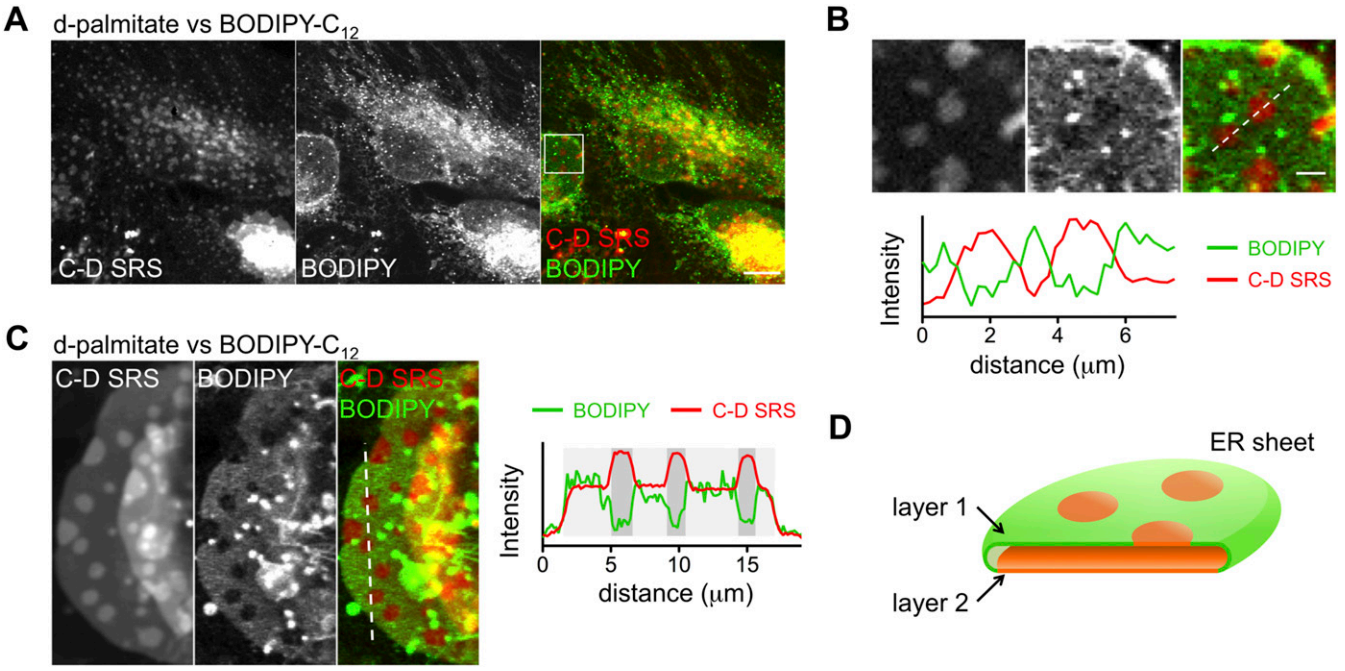

Fig. S5. Fluorescent membrane markers reveal lateral separation of palmitate-derived membrane domains. (*A*) HeLa cell was treated with d-palmitate and 1 μM BODIPY-C_{12} for 1 h. C–D SRS, BODIPY fluorescence, and their overlay are shown. (*B*) Magnified view is shown for the boxed area in *A*. Intensity profiles of the dashed line are shown below for both SRS (red) and fluorescence (green) channels. (*C*) Similar to Fig. 4*C*. (*D*) Illustration of lamellar ER cisternae and the proposed segregation between palmitate-derived domains (red) and the ER (green). Layer 2 is completely derived from palmitate, while layer 1 is ER membrane intercalated by palmitate-derived domains. (Scale bars: major, 10 μm; *Inset*, 2 μm.)

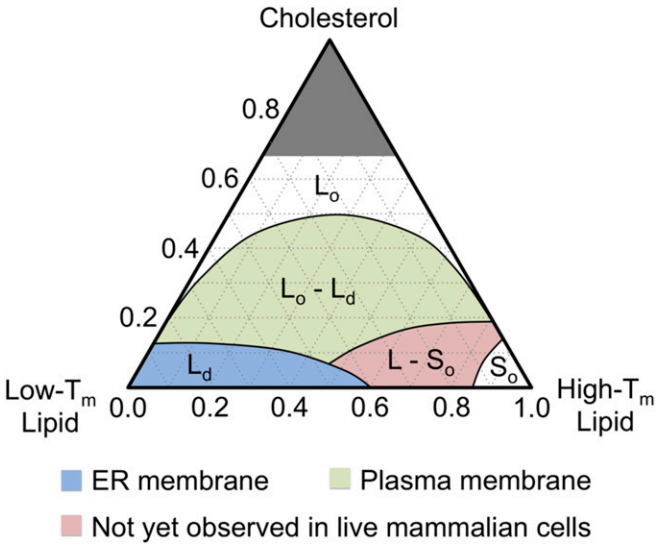

		order	diffusion
L_d	Liquid disordered	low	fast
L_o	Liquid ordered	high	fast
S_o	Solid ordered	high	slow

Fig. S6. Sketch of phase diagram of biomimicking ternary-component model membrane. Solid lines indicate phase boundaries defined by composition of each component in the mixture at a given temperature such as 37 °C. Phase regions are colored to show the current understanding of biological membrane phase and do not necessarily represent the exact composition. Area above 66% cholesterol exceeds its solubility in lipid bilayer, and thus is not considered here. Adapted from ref. 7.

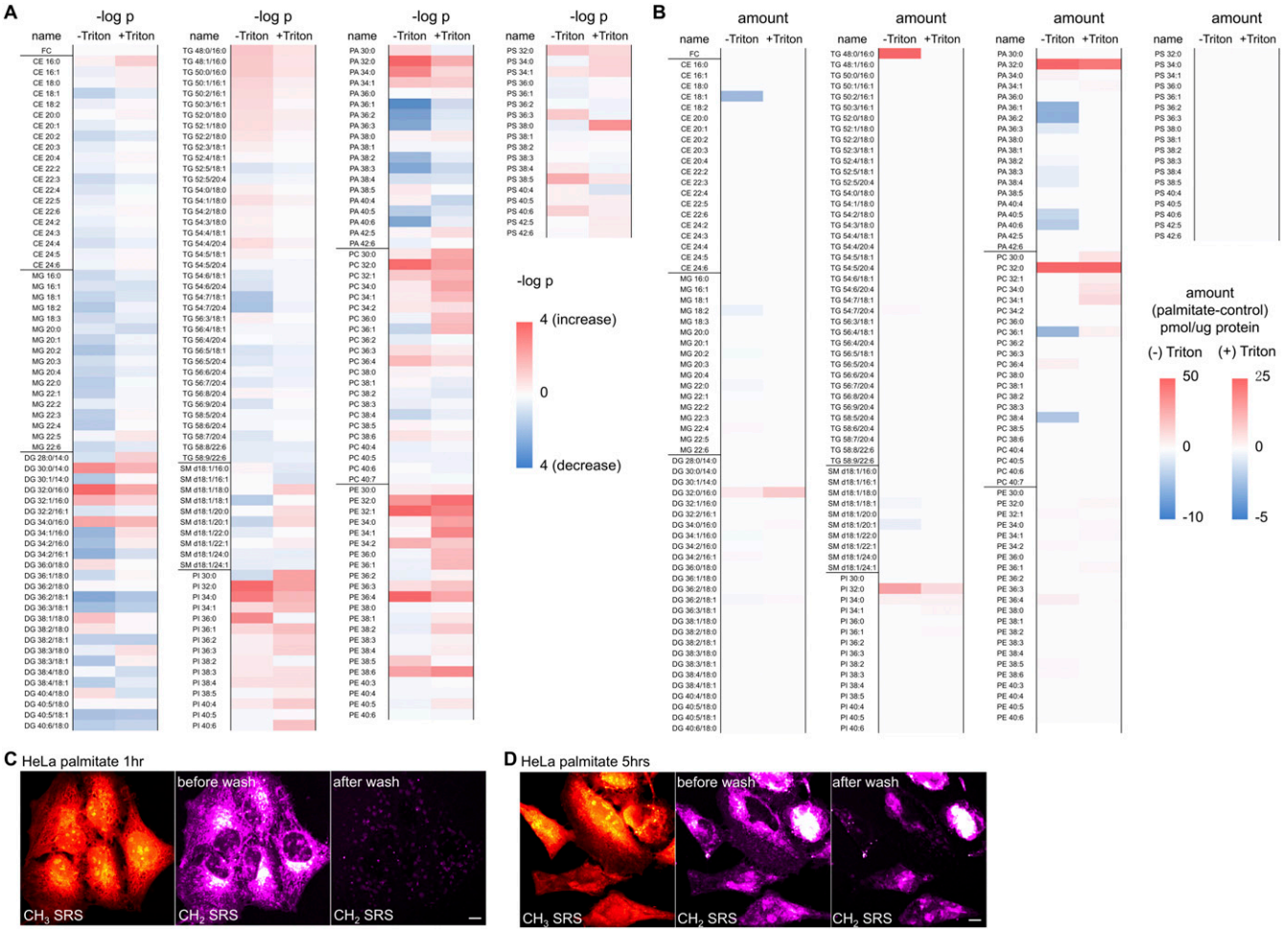

Fig. S7. (*A*) Log(p) value and (*B*) amount change in total lipid extract (−Triton) or detergent-resistant lipid fraction (+Triton) after palmitate treatment in HeLa cells for 5 h. (*C* and *D*) HeLa cells were treated with 400 μM palmitate for 1 h (*C*) or 5 h (*D*). Protein CH_3 and lipid CH_2 SRS signal were taken before and after extraction by 0.5% Triton X-100 for 10 min at 4 °C. Significant amount of lipid showed detergent resistance. (Scale bars: 10 μm.)

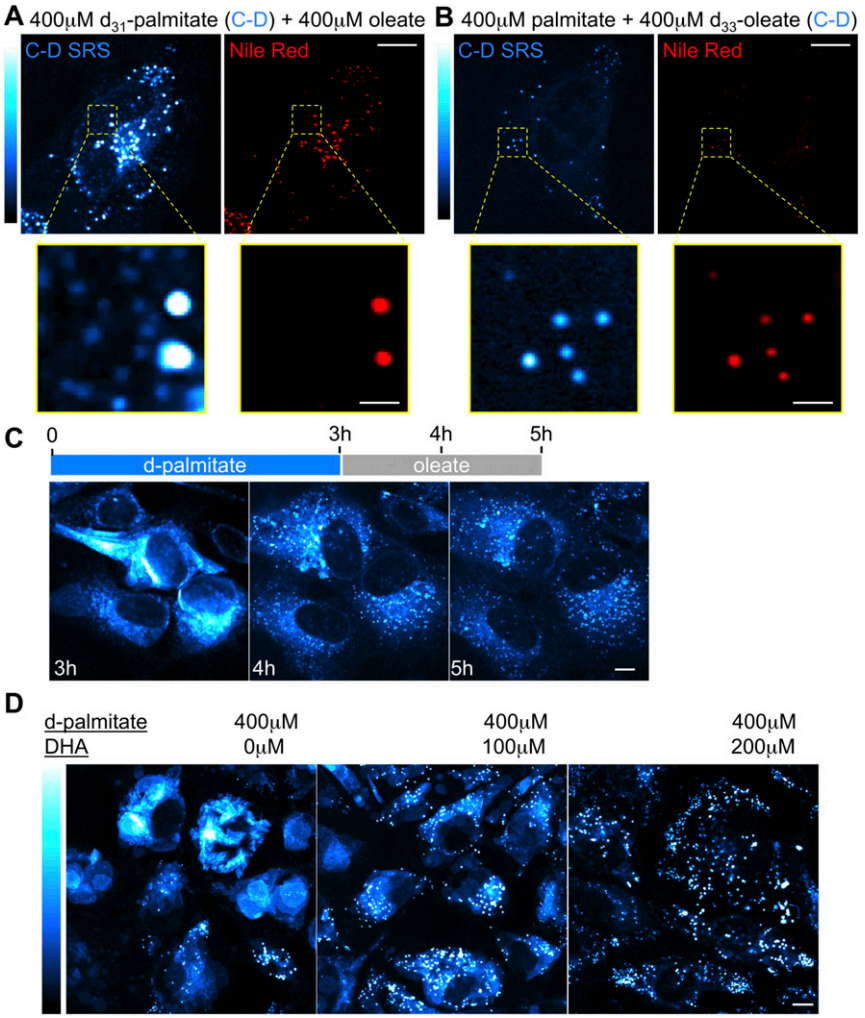

Fig. S8. UFAs are able to tune the formation of solid-like domain. (*A* and *B*) HeLa cells were treated with 400 μM palmitate and 400 μM oleate for 2 h, with isotope labeling on palmitate (*A*) or oleate (*B*), and then stained by Nile Red for LDs. *A* and *B* were adjusted to same contrast for visualizing non-LD compartment, and thus LDs appear saturated in intensity in *B*. (*C*) HeLa cells were treated by d-palmitate for 3 h to induce solid membrane formation. The medium was then changed to 200 μM oleate and time-lapse C–D SRS image was taken every 1 h. (*D*) C–D SRS images of HeLa cells treated with combination of d-palmitate and increasing concentrations of DHA. (Scale bars: major, 10 μm; *Inset* in *A* and *B*, 2 μm.)

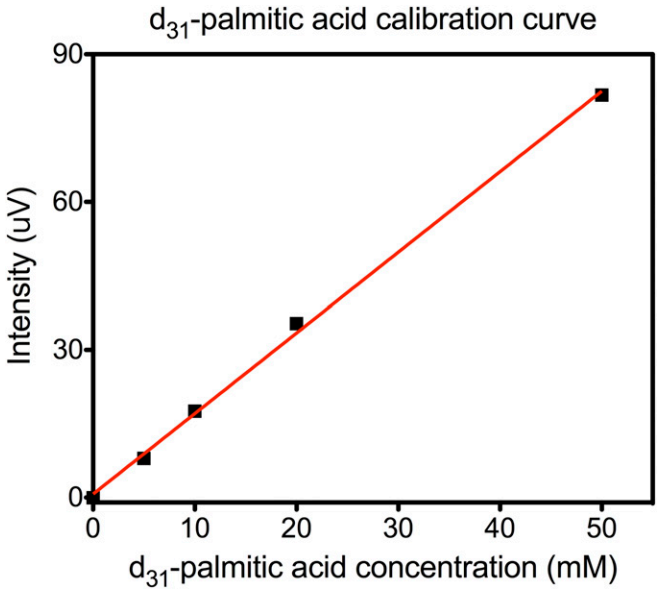

Fig. S9. Calibration curve for d-palmitic acid. SRS intensity is plotted against d-palmitic acid concentration (black) and then fitted with linear regression (red).

Table S1. Names and transition temperatures of related lipid species

Lipid species	Name	Acyl chain	Transition temperature (T_m/°C)*
PC	POPC†	C16:0/C18:1	−2
	DLPC	C12:0/C12:0	−1
	DMPC	C14:0/C14:0	24
	DPPC	C16:0/C16:0	41
	DSPC	C18:0/C18:0	55
	d_{62}-DPPC	C16:0/C16:0	37
PA	DMPA	C14:0/C14:0	50
	DPPA	C16:0/C16:0	67
PI	DPPI	C16:0/C16:0	41
DG	DPG	C16:0/C16:0	66

*Transition temperature data are adapted from refs. 6 and 8. Melting point is used instead of transition temperature for DAG.
†POPC was often used to model ER membrane in vitro.